International Journal of Automotive Technology, Vol. 21, No. 4, pp. 813−822 (2020)
DOI 10.1007/s12239−020−0079−7

pISSN 1229−9138/ eISSN 1976−3832

TEMPERATURE ANALYSIS OF WET CLUTCH SURFACES DURING CLUTCH ENGAGEMENT PROCESSES BASED ON FRICTION PAD PATTERNS

Jamin Kong[1)] and Siyoul Jang[2)*]

[1)]Graduate School of Automotive Engineering, Kookmin University, Seoul 02707, Korea
[2)]School of Automotive Engineering, Kookmin University, Seoul 02707, Korea

(Received 9 July 2019; Revised 26 September 2019; Accepted 2 October 2019)

ABSTRACT−Temperature distributions of wet clutch contact during engagement and disengagement processes are investigated considering lubricant flow behaviors in the gap between the friction pad and steel separator. Frictional heat generated by wet clutch contact in repeated operational modes that simulates high thermal endurance performance of a wet clutch system is modeled. This study applies CFD analysis to the lubricant convective flows that remove most of the frictional heat with respect to groove patterns on the frictional pad surface. Based on fluid flow analysis between the friction pad gap and the steel separator that includes the effects of pattern shapes on the friction pad, frictional heat, convective cooling behaviors and temperature distributions are computed with the repeated modes of varying sliding velocities and applied loads. The cooled frictional heat is investigated considering the convective flows in the gap of friction pad and separator. Frictional temperature variations on a wet clutch surface are computed for the effects of groove pattern shapes on the friction pad, waffle, and radial-arc types for better cooling effects. It is expected that the computational results will provide design methods for higher heat resistance durability and stable frictional torque transfer and effective cooling performance in wet clutch systems.

KEY WORDS : Wet clutch engagement, Frictional heat, Lubrication, Friction torque transfer, Friction pad patterns

NOMENCLATURE

A : area, m^2
C_p : specific heat coefficient, J/kgK
d : diameter, m
h : convective heat transfer coefficient, W/m^2K
h : lubricant film thickness, m
k : conductivity, W/mK
L : flow path length, m
P : pressure, N/m^2
Pr : Prandtl number, $C_p\mu/k$
R_n : contact radius, m
Re : Reynold's number, $\rho UL/\mu$
q : heat flux, W/m^2
r, θ : polar coordinate, m, rad
x, y, z : spatial coordinate, m
α : heat absorption ratio
η : viscosity, N/m^2s
μ_d : dynamic friction coefficient
Θ : temperature, °C
Θ_o : initial temperature, °C
ρ : density, kg/m^3
ω : rotational speed, rpm

SUBSCRIPTS

e : engine
c : clutch
F, F : friction face
F, G : friction pad groove
H, G : home groove
i : in
f : friction pad
n : grid element for computational domain
o : out
s : steel separator
so : surface on the lubricant volume
surf : surface
T, F : total face

1. INTRODUCTION

Recently, wet clutch mechanisms have been increasingly employed as automotive powertrains adopt high performance moving-off devices as well as various power distribution sources for higher fuel efficiency, such as P0 to P4 hybrid systems. Regardless of the wet clutch system's functions, such systems require high endurance performance and thermal stability in frictional torque controls. In the wet clutch pack, the lubricant should

*Corresponding author. e-mail: jangs@kookmin.ac.kr

remove frictional heat, which is strongly influenced by the pattern shapes on the friction pad. Therefore, it can control the friction coefficient above the necessary lower limit against increasing temperature. Thus, compared to dry clutch systems, the frictional torque transfer of wet clutch systems are widely used in high torque appliances (Yang *et al*., 1995).

A wet clutch operates in a sealed lubricant pack. In such a sealed pack, mechanical surface contact and lubrication occur simultaneously. As the engagement process starts, lubrication with viscous frictional torque begins to function. Then, as the lubricant film collapses with the applied load, mechanical contact between the friction pad and steel separator begins to generate mechanical frictional torque transfer. Many studies into frictional torque transfer in wet clutch systems have investigated the contact mechanisms of these two lubrication methods and direct mechanical contact (Berger *et al*., 1996; Marklund *et al*., 2007).

Frictional heat is inevitable in both wet and dry clutch systems. In a wet system, most frictional heat is removed by convective cooling of the lubricant fluid flow. Such flows are greatly influenced by the shape of the pattern on the friction pad during engagement and disengagement periods. Well-streamlined flows through the groove channels in the gap between the friction pad and the steel separator increase the flow rates and effectively help reduce increases in frictional temperature. In addition to contributing to effective convective cooling, the patterns on friction pads are intended to reduce drag torque in disengagement periods. Precise investigation of the effects of groove pattern shapes on lubricant flow behaviors requires very detail simulations with CFD analysis. Such investigations can provide favorable convective flow designs for effective cooling on the friction pad and steel separator (Zagrodzki, 1990; Jen and Nemecek, 2008; Xiaozeng *et al*., 2015; Cho *et al*., 2018; Mahmud *et al*., 2018).

Many studies have computed the increase in temperature in a wet clutch pack with a simple slip mode (Davis *et al*., 2000; Marklund *et al*., 2007; Jen and Nemecek, 2008). However, simulations should involve repeated engagement and disengagement processes in order to investigate methods to limit increasing temperature on friction pad and steel separator surfaces as well as in the sump oil. Such methods are very important engineering design criteria. The maximum bound of increasing temperature with repeated work cycles must be analyzed under conditions that simulate a real working environment. Each engagement and disengagement cycle must consider variations of applied load, relative sliding speed, and duration time etc. in transient modes (Berger *et al*., 1996; Davis *et al*., 2000).

In this study, flow behaviors of the lubricant in the gap between the friction pad and steel separator surface depending on the groove patterns are investigated using CFD analysis to identify design methods for effective convective heat cooling performance. Some groove patterns analyzed under repeated operating conditions are compared to identify groove patterns that yield better cooling performance in wet clutch systems.

2. MODELING WET CLUTCH CONTACTS

Modeling wet clutch contacts can be divided into two mechanisms, i.e., viscous shear contact and mechanical direct contact between the friction pad and steel plate. Frictional heat can be generated by both contact types. Mechanical contact generates greater amounts of frictional heat compared to viscous shear contact. On the other hand, viscous shear contact plays important roles when engagement first starts. In addition, viscous shear contact characterizes the μ-V friction property that is very important to reduce shudder vibration (Davis *et al*., 2000).

Although the wet clutch contact mechanism includes very complex phenomena relative to the permissible behavior of the lubricant into the friction pad solid, etc. (Berger *et al*., 1996; Davis *et al*., 2000), only the viscous flow behaviors between the friction pad and steel plate are investigated to identify the effect of convective cooling by lubricant flows during the engagement and disengagement processes in a wet clutch system.

In this study, two friction pad patterns are considered, i.e., the radial waffle (RW) type, which is used by most wet clutch systems, and the radial-arc (RA) type. The radial-arc

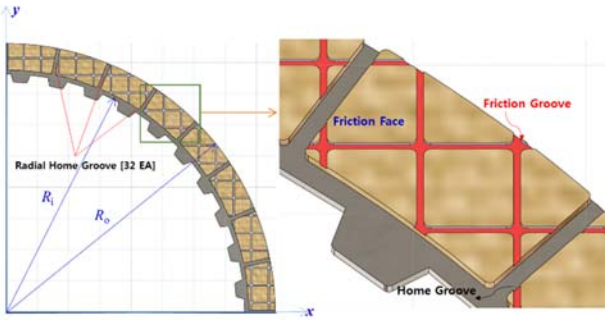

(a) Radial waffle (RW) pattern on friction pad

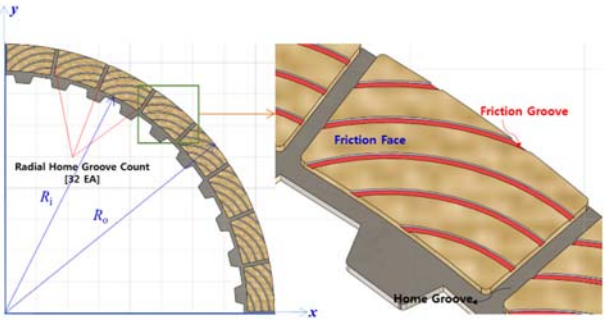

(b) Radial-arc (RA) pattern on friction pad

Figure 1. Friction pad pattern models.

Table 1. Clutch pads and lubricant parameters.

Items	Groove type		Friction pad	
Types	RW	RA	Density	1020 kg/m^3
Friction pad inner dia.	193.60 mm		Specific heat	1500 J/kgK
Friction pad outer dia.	215.00 mm		Thermal conductivity	0.261 W/mK
Friction pad thickness	0.78 mm		Core and separator plate	
Friction groove thickness	0.53 mm		Density	8030 kg/m^3
Core plate thickness	0.85 mm		Specific heat	502.48 J/kgK
Friction area (mm^2)	5400.25	5326.40	Thermal conductivity	46.04 W/mK
Friction area rate of change (%)	0	− 1.36	Fluid	
Separator plate inner dia.	192.80 mm		Density	846.67 kg/m^3
Separator plate outer dia.	216.80 mm		Specific heat	2177 J/kgK
Separator plate thickness	2.00 mm		Thermal conductivity	0.126 W/mK
Gap thickness@disengagement	0.25 mm		Viscosity	0.0264 kg/ms

type is newly purposed for favorable flow behaviors to the outside radius in order to enhance the convective cooling effects (Figure 1). To compare frictional heat generation and cooling performance, both types of patterns are designed to have nearly the same contact area. Detail dimensions and other properties of wet clutch pack are listed in Table 1.

The wet clutch contact models relative to frictional heat generation and release are shown in Figure 2. The models are based on wet clutch operation during engagement and disengagement processes. Frictional heat generation during these processes is explained relative to slip, engagement, and disengagement phases. In the engagement process, the clutch has a slip motion relative to the applied load (slip phase ⓐ, Figure 2 (a)), and finally the friction pad sticks to the steel separator with zero relative velocity (engaged phase ⓑ). The slip phase generates most of frictional heat. Here as well as being conducted to the friction pad and separator, some of the heat is simultaneously released by the lubricant convective flow.

A slip phase also occurs the moment that the engaged friction pad separates from the steel separator. During the engaged phase, frictional heat generation does not occur because the relative sliding velocity is zero. At this time, frictional heat is conducted to adjacent materials without generating heat, and some is done by convective flow through the grooves. The engaged phase is shown in Figure 2 (b).

The disengagement phase (ⓒ, Figure 2 (c)) occurs when the clutch pad and steel separator are in disconnected mode, i.e., with a relatively small gap of approximately ~ 0.25 mm. The generated heat is swept by flushed flows of the lubricant. Potentially large flow rates through the gap with favorable streamlined fluid flows by the groove patterns on the friction pad are required to obtain efficient cooling of the frictional temperature on the wet clutch surfaces.

A wet clutch operation mode that includes engagement and disengagement processes is shown in Figure 3 where the friction pad of transmission speed (ω_c) and separator speed of engine speed $\langle \omega_c \rangle$, and the duration of the applied pressure are shown.

2.1. Slip Phase Thermal Modeling

The frictional torque $T_{c,n}$ and induced heat flux q_{fric} on the area element of wet clutch pad and separator are computed by the product of the applied pressure P_n, relative sliding speed ($\omega_e - \omega_c$), friction coefficient μ_d, heat absorption ratio α_s, contact radius R_n, and contact area $A_{F,F}$, Equation (1) during the slip phase, as shown in Figures 2 and 3.

$$T_{c,n} = \mu_d A_{F,F} P_n R_n \times sgn(\omega_e - \omega_c) \tag{1}$$

$$q_{fric} = \alpha_s T_{c,n} \times (\omega_e - \omega_c) \tag{2}$$

The absorption ratios differ depending on the materials; thus, the friction pad α_f and steel separator α_s, absorption ratio is determined as follows (Berger *et al*., 1996; Mansouri *et al*., 2001; Jen and Nemecek, 2008):

$$\alpha_f = \frac{\sqrt{\rho_f c_{pf} k_f}}{\sqrt{\rho_s c_{ps} k_s} + \sqrt{\rho_f c_{pf} k_f}} \tag{3}$$

$$\alpha_s = \frac{\sqrt{\rho_s c_{ps} k_s}}{\sqrt{\rho_s c_{ps} k_s} + \sqrt{\rho_f c_{pf} k_f}} \tag{4}$$

where, ρ_f, ρ_s, C_{pf}, C_{ps}, k_f, and k_s are the density, specific heat, and conductivity for the friction pad and separator, respectively.

Considering the conducted heat flux to each side of contact surface $A_{F,F}$, the friction pad, and the steel separator, the total heat flux by frictional heat generation is expressed

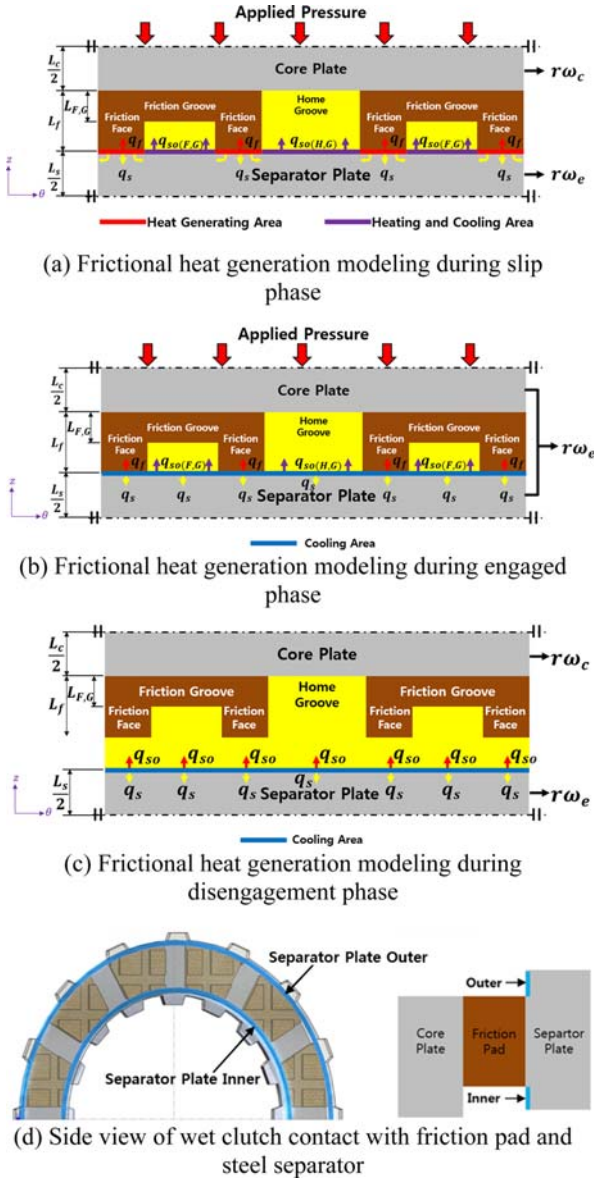

(a) Frictional heat generation modeling during slip phase

(b) Frictional heat generation modeling during engaged phase

(c) Frictional heat generation modeling during disengagement phase

(d) Side view of wet clutch contact with friction pad and steel separator

Figure 2. Frictional heat generation and cooling modes during engagement and disengagement periods in wet clutch system.

as follows.

$$q_{\text{surf(F,F)}} = q_{\text{fric}} - q_{\text{s(F,F)}} - q_{\text{f(F,F)}}$$
$$= T_{\text{c,n}} \times (\omega_{\text{e}} - \omega_{\text{c}}) - k_{\text{s}} A_{\text{F,F}} \frac{d\theta_{\text{F,F}}}{dz} - k_{\text{f}} A_{\text{F,F}} \frac{d\theta_{\text{F,F}}}{dz} \quad (5)$$

Therefore, the heat transfer distribution per unit area on the contacting surfaces of the friction pad and steel separator in the polar coordinate system can be described as follows.

$$\frac{1}{r_{\text{F,F}}} \frac{\partial}{\partial r_{\text{F,F}}} \left(k_{\text{s}} r_{\text{F,F}} \frac{\partial \theta_{\text{F,F}}}{\partial r_{\text{F,F}}} \right) + \frac{1}{r_{\text{F,F}}^2} \frac{\partial}{\partial \theta_{\text{F,F}}} \left(k_{\text{s}} \frac{\partial \theta_{\text{F,F}}}{\partial \theta_{\text{F,F}}} \right) +$$
$$\frac{q_{\text{surf(F,F)}}}{A_{\text{F,F}}} = \rho_{\text{s}} C_{\text{ps}} \frac{\partial \theta_{\text{F,F}}}{\partial t} \quad (6)$$

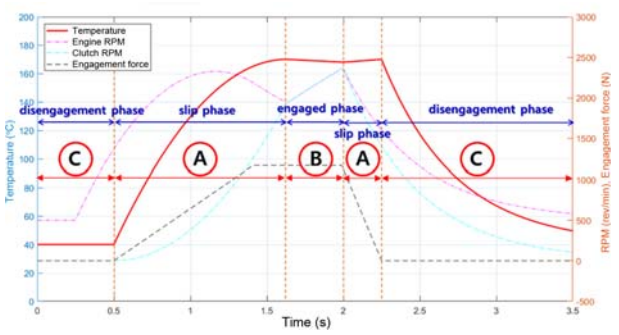

Figure 3. Operating phase modes of wet clutch engagement and disengagement processes as shown in Figure 2.

Figure 4. Meshes on the wet clutch surface for the computation of lubricant flow and temperature distribution.

Convective heat flows through the friction pad groove, the home groove, the gap between the friction pad and separator, and the inner and outer radius are expressed as follows:

$$q_{\text{so(F,G)}} = h_{\text{s(F,G)}} A_{\text{F,G}} (\theta_{\text{F,G}} - \theta_{\text{o}}) \quad (7)$$

$$q_{\text{so(H,G)}} = h_{\text{S(H,G)}} A_{\text{H,G}} (\theta_{\text{H,G}} - \theta_{\text{o}}) \quad (8)$$

$$q_{\text{so(in)}} = h_{\text{s(in)}} A_{\text{in}} (\theta_{\text{in}} - \theta_{\text{o}}) \quad (9)$$

$$q_{\text{so(out)}} = h_{\text{s(out)}} A_{\text{out}} (\theta_{\text{out}} - \theta_{\text{o}}) \quad (10)$$

where, $h_{\text{s(F,G)}}$, $h_{\text{s(H,G)}}$, $h_{\text{s(in)}}$, and $h_{\text{s(out)}}$ are the convection heat transfer coefficients, $A_{\text{F,G}}$, $A_{\text{H,G}}$, A_{in}, and A_{out} are the areas, and $\theta_{\text{F,G}}$, $\theta_{\text{H,G}}$, θ_{in}, and θ_{out} are the temperatures of the friction pad groove, the home groove, and the inner and outer radius, respectively. Note that θ_{o} is the initial temperature at each contact location.

Heat conductions through the friction and home grooves are combined with the convective heat flows of the lubricant in those grooves. The total heat flow in the friction groove, home groove, and inner and outer radius is expressed as follows.

$$q_{\text{s(F,G)}} = k_{\text{s}} A_{\text{F,G}} \frac{d\theta_{\text{F,G}}}{dz} \quad (11)$$

$$q_{\text{s(H,G)}} = k_{\text{s}} A_{\text{H,G}} \frac{d\theta_{\text{H,G}}}{dz} \quad (12)$$

$$q_{\text{s(in)}} = k_{\text{s}} A_{\text{in}} \frac{d\theta_{\text{in}}}{dz} \quad (13)$$

$$q_{s(out)} = k_s A_{out} \frac{d\theta_{out}}{dz} \tag{14}$$

$$q_{surf(F,G)} = q_{so(F,G)} + q_{s(F,G)}$$
$$= h_{s(F,G)} A_{F,G} (\theta_{F,G} - \theta_o) + k_s A_{F,G} \frac{d\theta_{F,G}}{dz} \tag{15}$$

$$q_{surf(H,G)} = q_{so(H,G)} + q_{s(F,G)}$$
$$= h_{s(F,G)} A_{H,G} (\theta_{H,G} - \theta_o) + k_s A_{H,G} \frac{d\theta_{H,G}}{dz} \tag{16}$$

$$q_{surf(in)} = q_{so(in)} + q_{s(in)}$$
$$= h_{s(in)} A_{in} (\theta_{in} - \theta_o) + k_s A_{in} \frac{d\theta_{in}}{dz} \tag{17}$$

$$q_{surf(out)} = q_{so(out)} + q_{s(out)}$$
$$= h_{s(out)} A_{out} (\theta_{out} - \theta_o) + k_s A_{out} \frac{d\theta_{out}}{dz} \tag{18}$$

In each grid point on the steel separator, temperature distributions by heat transfer are computed using the following equations in the polar coordinate system.

$$\frac{1}{r_{F,G}} \frac{\partial}{\partial r_{F,G}} \left(k_s r_{F,G} \frac{\partial \theta_{F,G}}{\partial r_{F,G}} \right) + \frac{1}{r_{F,G}^2} \frac{\partial}{\partial \theta_{F,G}} \left(k_s \frac{\partial \theta_{F,G}}{\partial \theta_{F,G}} \right) - \frac{q_{surf(F,G)}}{A_{F,G}} = \rho_s C_{ps} \frac{\partial \theta_{F,G}}{\partial t} \tag{19}$$

$$\frac{1}{r_{H,G}} \frac{\partial}{\partial r_{H,G}} \left(k_s r_{H,G} \frac{\partial \theta_{H,G}}{\partial r_{H,G}} \right) + \frac{1}{r_{H,G}^2} \frac{\partial}{\partial \theta_{H,G}} \left(k_s \frac{\partial \theta_{H,G}}{\partial \theta_{H,G}} \right) - \frac{q_{surf(H,G)}}{A_{H,G}} = \rho_s C_{ps} \frac{\partial \theta_{H,G}}{\partial t} \tag{20}$$

$$\frac{1}{r_{in}} \frac{\partial}{\partial r_{in}} \left(k_s r_{in} \frac{\partial \theta_{in}}{\partial r_{in}} \right) + \frac{1}{r_{in}^2} \frac{\partial}{\partial \theta_{in}} \left(k_s \frac{\partial \theta_{in}}{\partial \theta_{in}} \right) - \frac{q_{surf(in)}}{A_{in}} = C_{ps} \frac{\partial \theta_{in}}{\partial t} \tag{21}$$

$$\frac{1}{r_{out}} \frac{\partial}{\partial r_{out}} \left(k_s r_{out} \frac{\partial \theta_{out}}{\partial r_{out}} \right) + \frac{1}{r_{out}^2} \frac{\partial}{\partial \theta_{out}} \left(k_s \frac{\partial \theta_{out}}{\partial \theta_{out}} \right) - \frac{q_{surf(out)}}{A_{out}} = \rho_s C_{ps} \frac{\partial \theta_{out}}{\partial t} \tag{22}$$

2.2. Engaged Phase Thermal Modeling

As the phase of the engaged mode, heat transfer through contacting surfaces by conduction occurs without frictional heat generation, and some of the heat is removed by flushing the convective lubricant flow into the sump oil. The convection heat flows in the friction groove, home groove, and inner and outer are explained by Equations (7) ~ (10).

The temperature distribution on the steel separator is expressed in the polar coordinate system as follows:

$$\frac{1}{r_{F,F}} \frac{\partial}{\partial r_{F,F}} \left(k_s r_{F,F} \frac{\partial \theta_{F,F}}{\partial r_{F,F}} \right) + \frac{1}{r_{F,F}^2} \frac{\partial}{\partial \theta_{F,F}} \left(k_s \frac{\partial \theta_{F,F}}{\partial \theta_{F,F}} \right) - \frac{q_{surf(F,F)}}{A_{F,F}} = \rho_s C_{ps} \frac{\partial \theta_{F,F}}{\partial t} \tag{23}$$

where, $q_{surf(F,F)} = q_{s(F,F)} + q_{f(F,F)} + q_{so(total)} = k_s A_{F,F} \frac{d\theta_{F,F}}{dz} + k_f A_{F,F} \frac{d\theta_{F,F}}{dz} + q_{so(total)}$ and $q_{so(total)} = q_{so(F,G)} + q_{so(H,G)} + q_{so(in)} + q_{so(out)}$.

2.3. Disengagement Phase Thermal Modeling

At this phase of disengagement, convective cooling occurs by the lubricant flow through the grooves of the friction pad, home groove, and the gap between the friction pad and steel separator. Heat removed by convective flow of the lubricant on the surfaces of the friction pad and steel separator is expressed as follows.

$$q_{surf(T,F)} = q_{so(T,F)} + q_{S(T,F)}$$
$$= h_{s(T,F)} A_{T,F} (\theta_{T,F} - \theta_o) + k_s A_{T,F} \frac{d\theta_{T,F}}{dz} \tag{24}$$

Thus, the temperature distribution in the disengagement phase is expressed as follows.

$$\frac{1}{r_{T,F}} \frac{\partial}{\partial r_{T,F}} \left(k_s r_{T,F} \frac{\partial \theta_{T,F}}{\partial r_{T,F}} \right) + \frac{1}{r_{T,G}^2} \frac{\partial}{\partial \theta_{T,F}} \left(k_s \frac{\partial \theta_{T,F}}{\partial \theta_{T,F}} \right) - \frac{q_{surf(T,F)}}{A_{T,F}} = \rho_s C_{ps} \frac{d\theta_{T,F}}{dt} \tag{25}$$

2.4. Convective Heat Transfer Coefficients

The convective heat transfer coefficients are obtained at the locations of the friction groove (FG), home groove (HG), and the gap between the friction pad and separator as follows (Xiaozeng *et al*., 2015).

In the HG, the convective heat transfer coefficients are calculated as follows:

$$h_{s(H,G)} = \begin{cases} 1.86 \frac{k_o}{2R_n} \left(\frac{Re_{H,G} Pr}{l_{H,G}/d_e} \right)^{1/3}, & Re \le 500 \\ 0.064 \frac{k_o}{2R_n} Re_{H,G}^{0.8} Pr^{0.4}, & Re \ge 500 \end{cases} \tag{26}$$

where, k_o, $Re_{H,G}$, and Pr are the conductivity of the lubricant, Reynolds' number in the HG, and the Prandtl number, respectively.

In both the FG and the gap between the friction pad and the separator, the convective heat transfer coefficient is calculated as follows.

$$h_{s(F,F),(F,G)} = 0.332 \frac{k_o}{R_n} Re_{(F,F)(F,G)}^{0.5} Pr^{1/3}, \quad Re \le 5 \le 10^5 \tag{27}$$

In the inner and outer locations on the separator, the convective heat transfer coefficient is computed as follows.

$$h_{s(in),(out)} = 0.4193 k_o (Re_{(in),(out)})^{0.618} \frac{Pr^{1/3}}{d_{in,out}}, \quad Re \le 1.5 \le 10^5 \tag{28}$$

All convective heat transfer coefficients (Figure 5) are obtained using CFD analysis (FLUENT) for the velocity values in the Reynolds' number computation, and these are

the variables by relative sliding speeds and temperatures depending on the groove patterns. A detailed CFD analysis shows that the convective heat transfer coefficients are dependent on the sliding speed, the clutch working phases (engagement and disengagement), and the lubricant temperature for the two friction pad patterns (waffle and radial-arc patterns).

To obtain the fluid flow behaviors for the convective heat transfer coefficients that include Reynolds' number, two-phase CFD analyses were performed for the fluid velocity and volume fraction of the lubricant in the gap space of a wet clutch. Fluid flow behaviors vary depending on the friction pad patterns, which leads to different cooling performance. This study investigated the flow behaviors for the waffle and radial-arc friction pad patterns with two-phase flow analysis to precisely identify the effects of friction pad patterns on cooling performance.

The conditions for the friction pad contact shape, inlet flow rate, and other working conditions during the engagement and disengagement phases are shown in Figure 6. The relative sliding speeds (500 ~ 2500 rpm) between the friction pad and steel separator are assigned under the conditions of the launching gear ratio. The database of fluid behaviors, such as velocity fields and Reynolds' numbers, for each friction pad pattern by two-phase fluid analysis are stored for the convective heat transfer coefficient computation. These are used to compute the convective heat transfer coefficient, which is required in the computation of the temperature distributions on the steel separator. A comparison of the selected velocity fields fluid in the waffle and radial-arc patterns is shown in Figure 7.

The velocity fields in radial-arc type are more aligned to the groove patterns. In the waffle pattern, they are distributed more randomly; thus, the convective flow through the outlet of the outer radius is more activated. This leads to enhancement of cooling performance by the groove patterns on the friction pad under the same

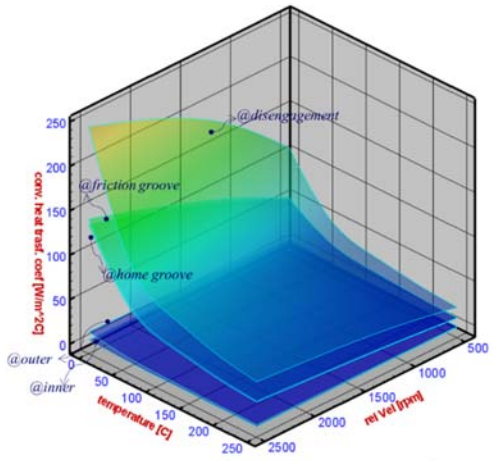

(a) Convective heat transfer coefficient map of the RW type

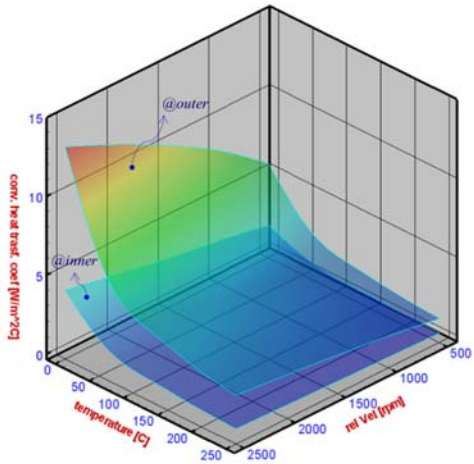

(b) Enlarged view of convective heat coefficient maps in inner and outer parts of the RW type pattern

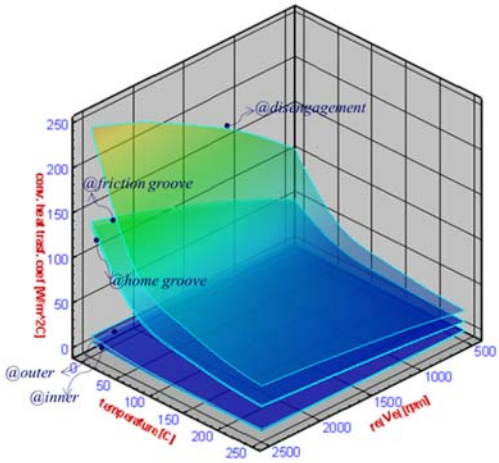

(c) Convective heat transfer coefficients of the RA type

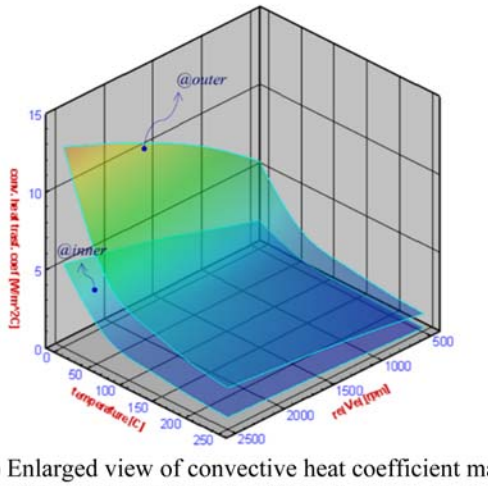

(d) Enlarged view of convective heat coefficient maps in inner and outer parts of the RA type pattern

Figure 5. Convective heat transfer coefficients of the RW and RA type patterns.

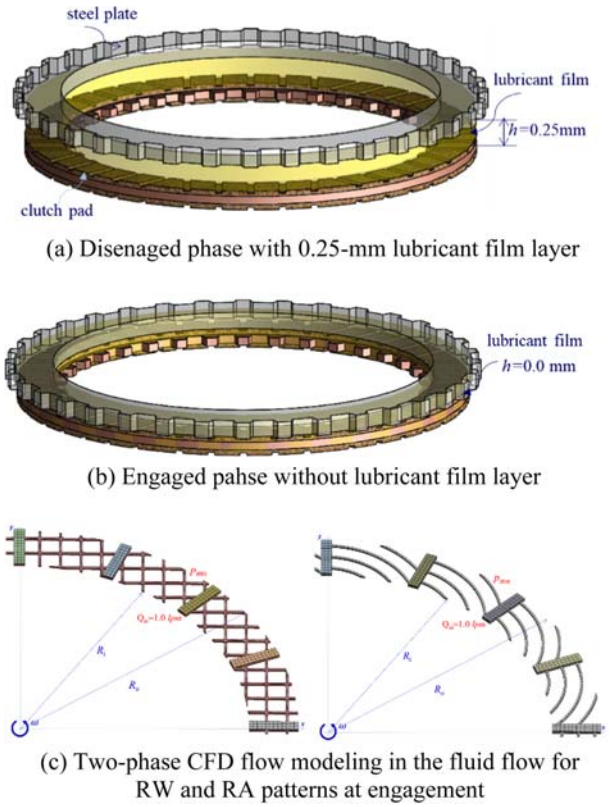

(a) Disenaged phase with 0.25-mm lubricant film layer

(b) Engaged pahse without lubricant film layer

(c) Two-phase CFD flow modeling in the fluid flow for RW and RA patterns at engagement

Figure 6. Two-phase flow behaviors in gap between friction pad and steel separator at engagement and disengagement and CFD modeling for RW and RA types.

operating conditions. The velocity fields obtained by CFD analyses are used in the thermal behaviors of the wet clutch contact surfaces during either the engagement or disengagement processes (Figure 7).

3. TEMPERATURE DISTRIBUTIONS ON WET CLUTCH CONTACT

After computing the behaviors of the lubricant flows with two-phase CFD analysis, the temperatures were investigated relative to the maximum values over the temperature distributions on the contact surface of the steel separator which has higher conductivity than friction pad and generates more hot spots on its own surface. Repeated engagement and disengagement modes with varying relative sliding velocities and applied loads, which simulate the endurance test modes of the wet clutch system as in vehicle launching, were imposed on the wet clutch operation. The maximum temperature distributions were compared to the proposed waffle and radial-arc friction pad patterns. The detailed driving mode of the wet clutch operation is shown in Figure 8 and described in Table 2.

The temperature distribution on the steel separator and its variations during wet clutch engagement were computed for the waffle (Figure 9) and radial-arc types

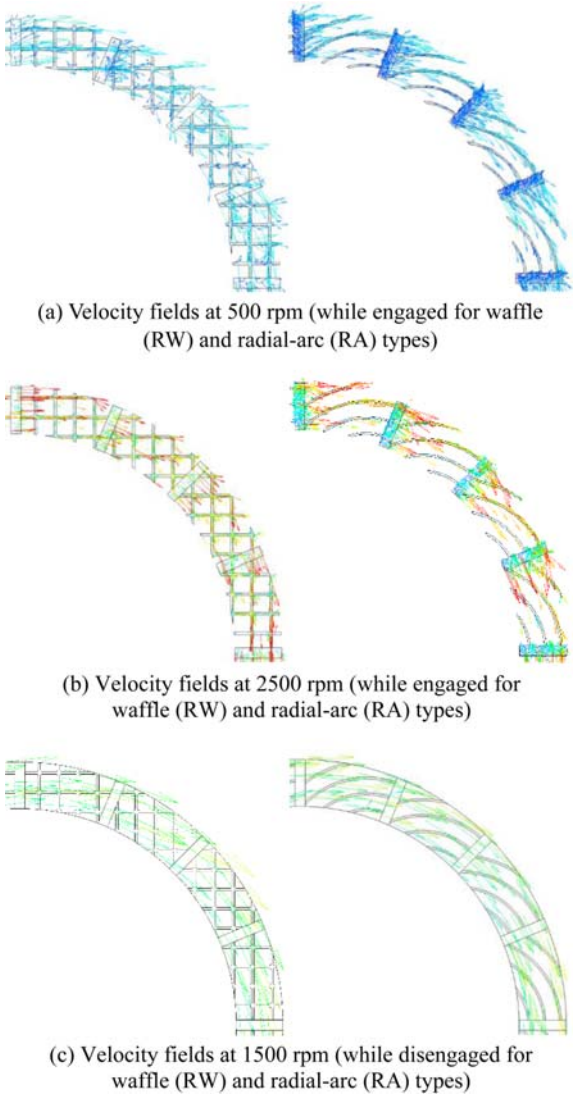

(a) Velocity fields at 500 rpm (while engaged for waffle (RW) and radial-arc (RA) types)

(b) Velocity fields at 2500 rpm (while engaged for waffle (RW) and radial-arc (RA) types)

(c) Velocity fields at 1500 rpm (while disengaged for waffle (RW) and radial-arc (RA) types)

Figure 7. Flow patterns of lubricant in clearance gap of wet clutch depending on sliding speeds during engagement and disengagement phases.

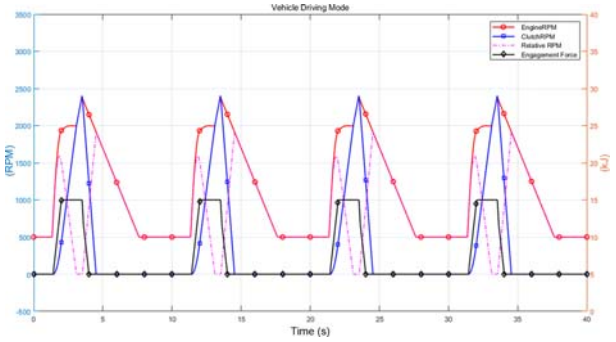

Figure 8. Wet clutch driving mode in four cycles.

(Figure 10). As can be seen, the temperature on the contact surface of the waffle type shows higher distributions than on the radial-arc type at the final stage of the slip phase of

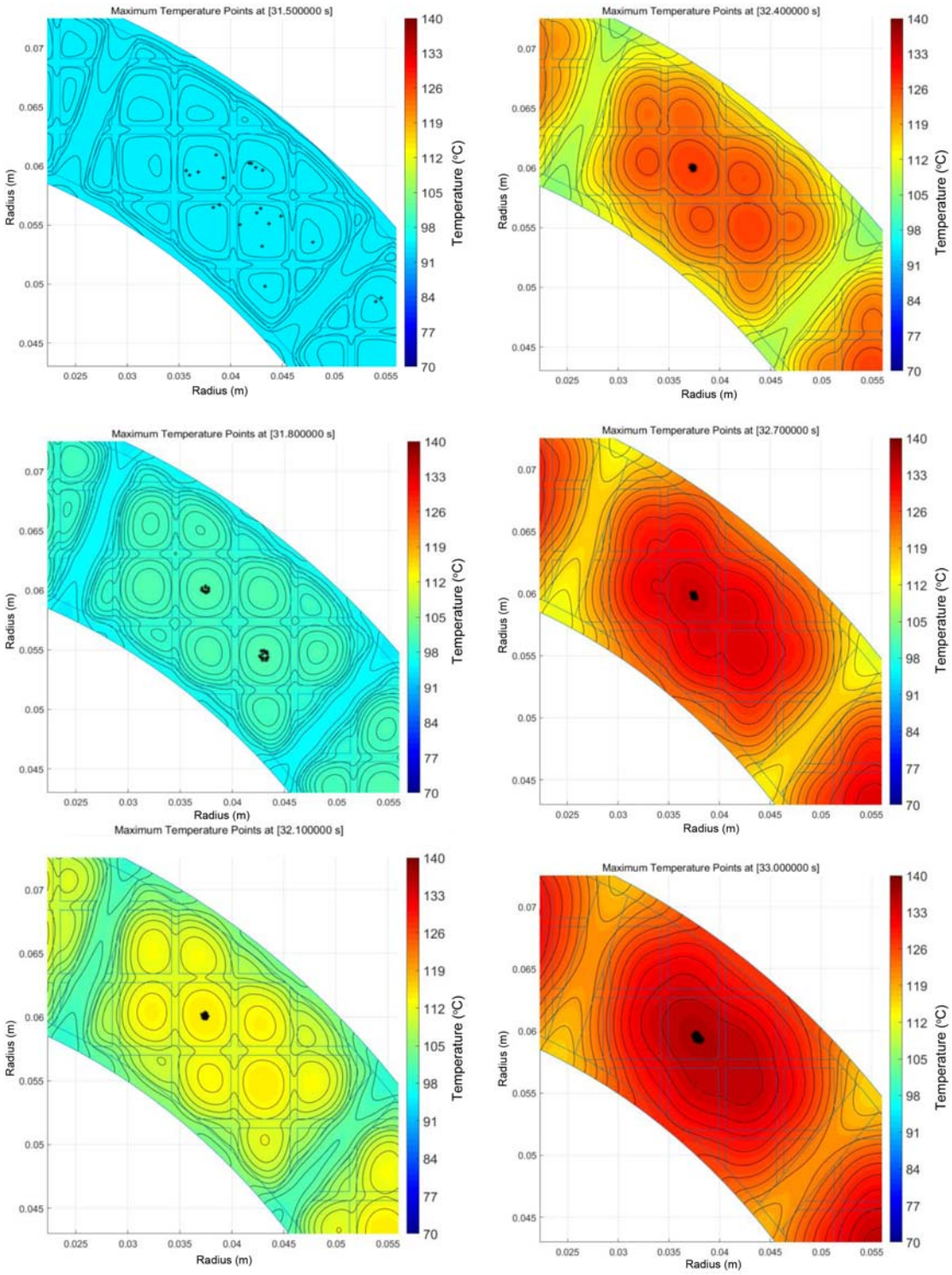

Figure 9. Maximum temperature for waffle type (RW) at 31.5, 31.8, 32.1, 32.4, 32.7, and 33.0 second.

the repeated four-cycle engagement mode. This means that cooling by convective flow with the friction pad patterns is performed more effectively in the radial-arc type, which was designed to realize streamlined flow behaviors along the FG. The maximum temperature variations on the contacting steel separator are compared in Figure 11, which shows that the radial-arc type pattern has a lower temperature increase by frictional heat than the waffle pattern pad. The friction pad patterns by streamlined lubricant behaviors enhance the convective cooling

Table 2. Vehicle Driving Conditions.

Vehicle driving conditions	
Cycles	4
Total time for four cycles	40 s
Slip time for one cycle	1.65 s
Disengagement time for one cycle	7.84 s
Maximum engagement force	1000 N
Frictional energy per cycle	20.73 kJ

performance and provide a smaller temperature increase, which results in stable frictional torque transfer.

4. CONCLUSION

In this study, the temperature distribution on the steel separator contacting a friction pad in a wet clutch system was computed during repeated engagement and disengagement operating cycles with friction pad patterns. The results show that the proposed waffle and radial-arc

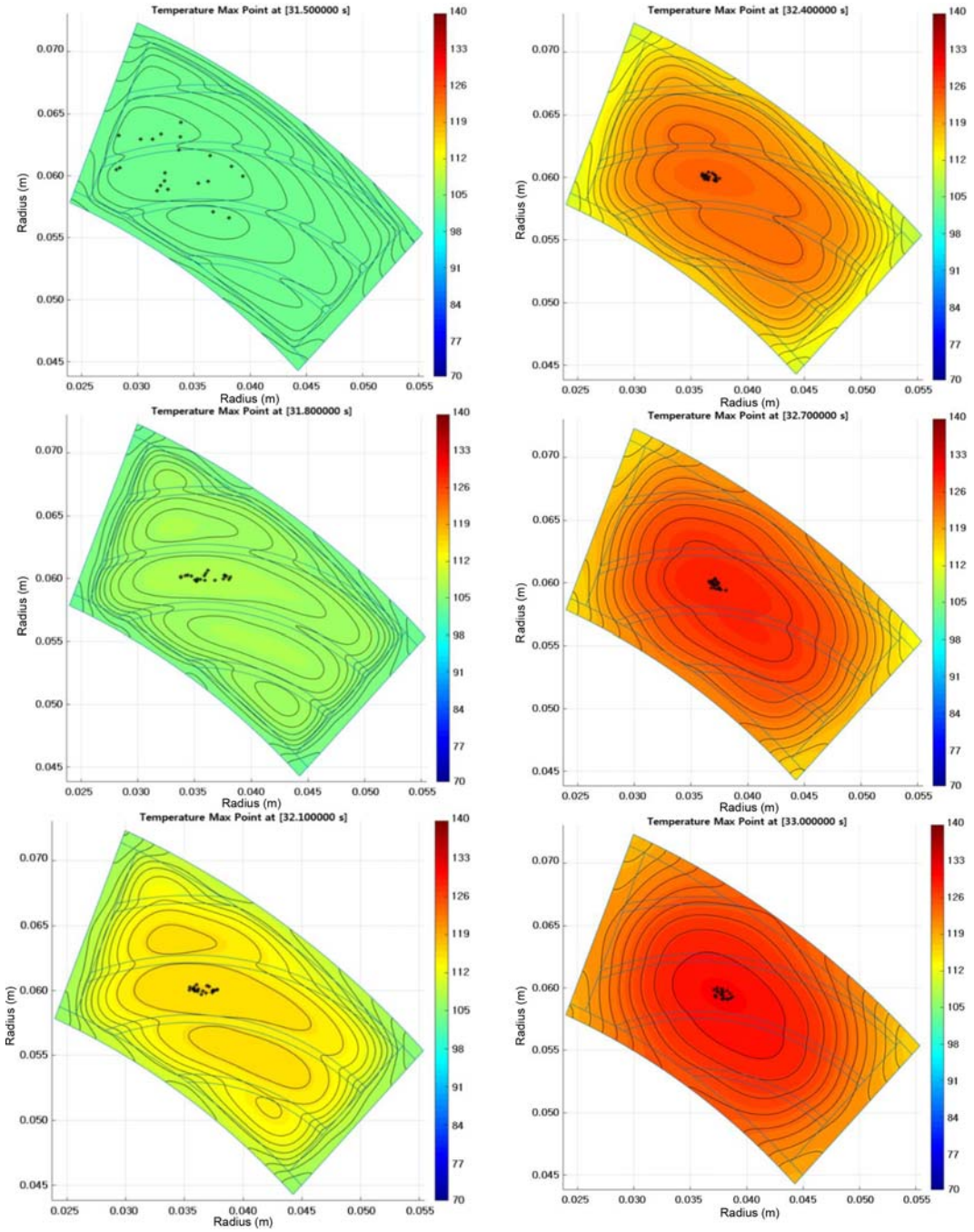

Figure 10. Maximum temperature points for radial-arc (RA) type at 31.5, 31.8, 32.1, 32.4, 32.7 and 33.0 second.

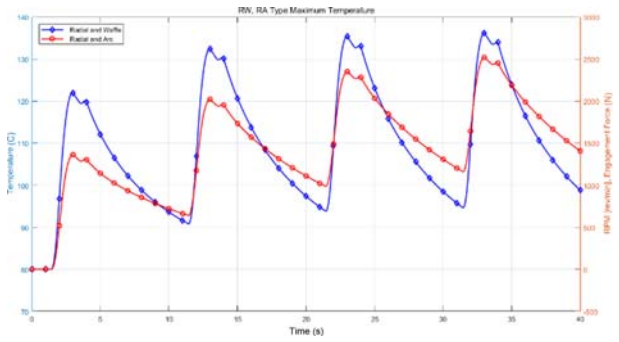

Figure 11. Comparison of maximum temperature on the steel plate surface during repeated engagement and disengagement operations of vehicle launching mode with waffle (RW) and radial-arc (RA) friction pad patterns.

patterns yield a higher convective cooling effect. This is intended to realize efficient cooling performance for the wet clutch pad under the same operating conditions.

The radial-arc pattern was designed for favorable flow behaviors with the rotation of the wet friction pad. The computational results demonstrate that this friction pad pattern generates more convective lubricant flows, which takes more frictional heat energy than the conventional waffle pattern. These results help us understand the cooling mechanism in wet clutch system and provide a design method for wet friction pad patterns with better cooling capability.

ACKNOWLEDGEMENT–This research was supported by the program of Clutch System Collaborative Research Center, Kookmin University-Transmission Research Lab. HYUNDAI MOTOR GROUP and basic research program of NRF #2018R1D1A1B07043950.

REFERENCES

Berger, E. J., Sadeghi, F. and Krousgrill, C. M. (1996). Finite element modeling of engagement of rough and grooved wet clutches. *J. Tribology* **118**, **1**, 137–146.

Cho, J., Jang, S., Kim, W. and Lee, Y. (2018). Wet single clutch engagement behaviors in the dual-clutch transmission system. *Int. J. Automotive Technology* **19**, **3**, 463–472.

Davis, C., Sadeghi, F. and Krousgrill, C. (2000). A simplified approach to modeling thermal effects in wet clutch engagement: Analytical and experimental comparison. *J. Tribology* **122**, **1**, 110–118.

Jen, T. C. and Nemecek, D. J. (2008). Thermal analysis of a wet-disk clutch subjected to a constant energy engagement. *Int. J. Heat and Mass Transfer* **51**, **7-8**, 1757–1769.

Mahmud, S., Pahlovy, S. and Ogawa, M. (2018). Simulation to estimate the output torque characteristics and temperature rise of a transmission wet clutch during the engagement process. *SAE Paper No*. 2018-01-0402.

Mansouri, M., Holgerson, M., Khonsari, M. M. and Aung, W. (2001). Thermal and dynamic characterization of wet clutch engagement with provision for drive torque. *J. Tribology* **123**, **2**, 313–323.

Marklund, P., Maki, R., Larsson, R., Hoglund, E., Khonsari, M. M. and Jang, J. (2007). Thermal influence on torque transfer of wet clutches in limited slip differential applications. *Tribology Int*. **40**, **5**, 876–884.

Xiaozeng, X., Dongyue, Q., Fanbing, L. and Qingyu, W. (2015). Thermal-structural coupling analysis of wet clutch friction discs based on APDL. *Proc. 8th Int. Conf. Intelligent Computation Technology and Automation*, Nanchang, China.

Yang, Y., Lam, R. C., Chen, Y. F. and Yabe, H. (1995). Modeling of heat transfer and fluid hydrodynamics for a multidisk wet clutch. *SAE Paper No*. 1995-02-01.

Zagrodzki, P. (1990). Analysis of thermomechanical phenomena in multidisk clutches and brakes. *Wear* **140**, **2**, 291–308.